Dielectric Properties of Polypropylene Containing Nano-Particles

Bamji, S. S.; Abou-Dakka, M.; Bulinski, A. T.; Utracki, L.; Cole, K.

Publisher's version / la version de l'éditeur:
2005 Annual Report Conference on Electrical Insulation and Dielectric Phenomena, pp. 166-170, 2005-10-16

Web page / page Web
http://dx.doi.org/10.1109/CEIDP.2005.1560647
http://nparc.cisti-icist.nrc-cnrc.gc.ca/npsi/ctrl?action=rtdoc&an=15884114&lang=en
http://nparc.cisti-icist.nrc-cnrc.gc.ca/npsi/ctrl?action=rtdoc&an=15884114&lang=fr

Dielectric Properties of Polypropylene Containing Nano-Particles

S.S. Bamji, M. Abou-Dakka, and A.T. Bulinski
Institute for National Measurement Standards
National Research Council Canada
Ottawa, Ontario, Canada, K1A 0R6

L. Utracki and K. Cole
Industrial Materials Institute
National Research Council Canada
Boucherville, Quebec, Canada, J4B 6Y4

Abstract: A thermoplastic such as polypropylene reinforced with small quantities (<5% by weight) of nano-sized particles could show reduced flammability as well as improved dielectric properties. This paper describes short-term dielectric properties of polypropylene containing 0%, 2%, and 4% by weight of dispersed organosilicates. Ac and dc breakdown strength, tanδ, electroluminescence emission, and space charge distribution due to ac poling of polypropylene with and without the nanoparticles are reported.

Introduction

Polypropylene (PP) is extensively used as a dielectric material in power capacitors and cable wraps, as well as in layer and phase separators for rotating electrical equipment and transformers [1, 2]. It has excellent mechanical, thermal, and electrical properties and provides outstanding resistance to moisture, grease, and oils. PP does not present stress-cracking problems and compared to polyethylene it offers excellent electrical and chemical resistance at higher temperatures.

Incorporation of nanoparticles in a polymer matrix could provide dielectrics with new and improved properties. A thermoplastic such as PP could be reinforced with small quantities (<5% by weight) of nanoparticles. This could enhance the mechanical properties and flame resistance and may improve dielectric properties, such as long-term electrical breakdown strength, surface and volume conductivity and resistance to partial discharges.

This paper describes dielectric properties of PP during short-term electrical aging and compares them with PP containing dispersed nanoparticles. Breakdown strength, dielectric loss at power frequency, electroluminescence emission, and space charge distribution in these materials are compared and discussed.

Experimental

Sample Preparation: Three materials, isotactic PP with 0, 2, and 4-wt% of organosilicate, referred to in this text as PP-0%, PP-2%, and PP-4%, were used. The manufacture of polypropylene containing nanoparticles involved two new methods:

(1) Melt compounding of PP (ProFax PDC 1274 from Basell), with a 1:1 mixture of two compatibilizers [PP grafted with maleic-anhydride (PP-MA) from Eastman (Epolene-3015) and from Crompton (Polybond 3150)] and organoclay (Cloisite 15A, C15A, from SCP). The compounding was carried out under a blanket of dry nitrogen in a twin-screw extruder with a gear pump and an extensional flow mixer (EFM, gap = 63.5 μm, throughput Q = 10 kg/h) at 200°C. The resulting composition was: 88-wt%PP + 8-wt%PP-MA + 4-wt%C15A (referred to as PP-4%). The organoclay dispersion of PP-4% was characterized by X-ray diffraction (XRD) and high-resolution transmission electron microscopy (HRTEM). The interlayer spacing was d_{001} = 3.25 nm; the number of clay platelets in residual stacks N = 3.25, and the degree of exfoliation = 79%, i.e., 11% above that observed for extrusion without the EFM.

(2) The same materials were melt compounded using a combination of a single screw extruder and EFM (with 15 μm gap, 10 kg/h throughputs) at 180°C, under blanket of dry nitrogen. The composition of the compound was 92-wt%PP + 4-wt%PP-MA + 2-wt%C15A (referred to as PP-2%). The organoclay dispersion of PP-2% was characterized by XRD and HRTEM. The measured dispersion parameters were: d_{001} =3.45 nm, N = 2.64, and degree of exfoliation 20% above that observed for extrusion without EFM.

The three materials were molded using a hot press at 210°C under a pressure of 50 MPa to produce flat sheets having a thickness of 80±5 μm and 155±5 μm. The thinner samples were used to determine the light transmission characteristics, and then they were subjected either to ac or dc breakdown tests or used for tanδ measurements. The thicker samples had each of

their sides sputtered with gold electrodes having a diameter and thickness of 25 mm and 30 nm respectively and then used for electroluminescence and PEA measurements.

UV-VIS-NIM Spectra: The light transmission spectra of each of the three materials were obtained with a UV- VIS-NIR Perkin-Elmer spectrometer having a range of 160 nm to 3200 nm.

Breakdown (BD) Tests: The samples were placed between two electrodes inside an oil bath. The bottom circular electrode having a diameter larger than that of the sample was held at ground potential. The top electrode, connected to a high voltage supply, had a diameter much smaller than that of the sample so that several breakdowns could be obtained on each sample. For dc tests the positive voltage was increased at a rate of 90 V/s, while for ac tests the voltage was increased at a rate of 70 V/s till breakdown occurred. RMS values of ac voltage and field are used throughout this paper.

Tanδ and Capacitance: Andeen Hagerling Ultra-precision Capacitance Bridge operating at 15 V, 60 Hz was used to obtain tanδ and measure the capacitance of each sample.

Electroluminescence (EL): The setup for EL has been previously described [3]. An optical system was designed to capture EL from each sample subjected to ac voltage under uniform field geometry. Light emitted from only the central region of the sample was detected by a PMT operating in photon counting mode. EL emitted at any phase, from 0 to 360°, during each cycle of the ac voltage could be detected by the system. The electric field was increased from 0 to 40 kV/mm in steps of 2 kV/mm.

Phase Resolved PEA Technique: Space charge distribution in the sample during ac aging was obtained with a PEA system from FiveLabs, Japan. A constant pressure was maintained during the measurement and the spatial resolution of the system was ~10 μm. The sample was electrically stressed with ac voltage and special software was developed to synchronize the pulse generator with the high voltage supply to provide a train of 5 ns pulses during any phase angle, between 0 to 360°, of the ac voltage. The pulses with amplitude of 200 V were applied for 1000 consecutive cycles of the ac voltage. The average of several hundred repetitive measurements was obtained to improve the signal to noise ratio. The PEA signal was digitized at a rate of 10 GS/s by a fast digital oscilloscope and each data point was resolved at 100 ps.

Results and Discussion

The optical transmission of the three materials in the 160-3200 nm range is shown in Fig. 1. Between 200 nm and 300 nm (see inset) the transmission decreases as the nanoparticle content increases. This could be attributed to silicate and intercalate used in the nanocomposites. The apparent gradual decrease in transmission as the wavelength decreases from 2200 to 300 nm is mainly related to scattering, which increases as the wavelength gets closer to the dimensions of the scattering clay platelets. Much of the scattered light may actually be transmitted, but because it falls outside of the angle detected by the spectrometer, it appears as loss of transmission (or caused by absorption). For wavelengths above ca. 300 nm the scattering is significantly higher for PP-0% than for the nanocomposites, and this is almost certainly related to the size of the PP crystalline domains (spherulites). The spherulites have a different index of refraction from the amorphous regions, which leads to reflection of light at the interface and hence to scattering. The organoclay acts as a nucleating agent; hence it increases the number of spherulites and reduces their size, which shifts the scattering drop-off to shorter wavelength. In the near IR, the peak at 2750 nm arises from the fundamental OH stretching vibration of the hydroxyl groups contained within the silicate layers. As expected, its intensity is proportional to the amount of clay.

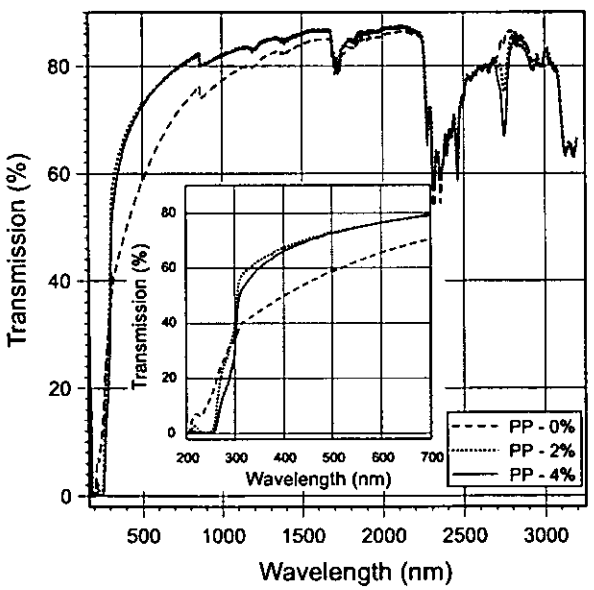

Fig. 1. UV-VIS-NIR transmission spectra of polypropylene containing 0, 2, and 4% by weight of organoclay.

The dc and ac BD strength of the three materials and the error of measurements are presented in Fig. 2.

The graph shows the average value of at least ten breakdowns for each material. Adding organoclay to PP increases the dc breakdown strength. Silicate layers are known to be efficient nucleating agents for crystallization of PP matrix. Charges could be trapped at the nanofiller-polymer matrix interfaces and thus decrease the probability of breakdown. For the three materials tested in this work, PP-2% had the highest breakdown strength, as shown in Fig. 2. The slightly lower ac and dc BD strength of PP-4%, as compared to PP-2%, could be due to the decrease in spherulite size and density and poorer dispersion of the nanoparticles.

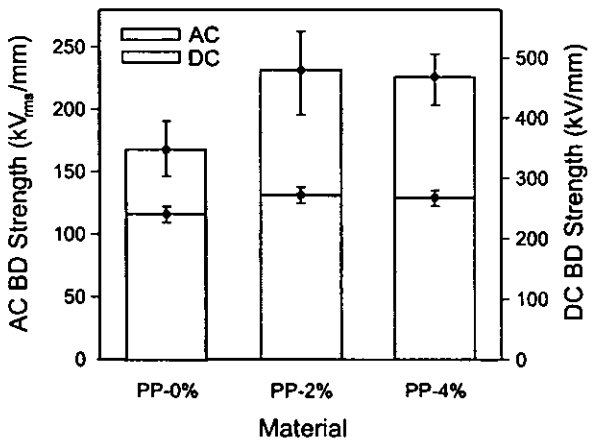

Fig. 2. AC and DC breakdown values of PP containing 0, 2, and 4% of nanoparticles

Tanδ and capacitance values at 15 V and 60 Hz of the three materials are listed in Table 1. Adding organoclay increases the tanδ of PP by an order of magnitude and PP-4% has twice the value of PP-2%. The capacitance also increases with the concentration of the nanofiller content. In the maleated PP the maleic anhydride groups are partially hydrolyzed, thus acidic and highly polar. The organoclay is montmorillonite with Fe^{+3} in the octahedral layer, and negative charges on the surface, ionically bonded to ammonium intercalant [4].

Table1. Tanδ and Capacitance values of PP, with and without nanofillers.

Material	Tanδ (x10^{-4})	Capacitance (pF)
PP-0%	1.88	123.33
PP-2%	20.1	138.97
PP-4%	42.8	146.70

According to molecular modeling the charge is highly delocalized, thus again polar, with the degree of polarity expected to be frequency dependent. These polar species increase the loss factor of the nanocomposites.

Fig. 3 shows typical EL emission from the three materials subjected to ac voltage. At least five samples of each material were tested. Adding organoclay to PP does not increase the EL inception field (~18 kV/mm) but, compared to PP-0%, the EL intensity was usually lower in PP-2% and higher in PP-4%. At low electric field, EL emission in polyolefin is caused by the recombination of electrons and holes injected into the insulating material subjected to ac voltage [3]. Enone and poly-(enone) sequences have been identified as luminescent centers in PP [5]. These polar species have equal affinity for electrons and holes and act as recombination centers for the charges of both polarities injected into the material. In the nanocomposites, the nanoparticles could provide additional recombination centers and this would increase the intensity of EL emission as in PP-4%. However, the EL intensity of PP-2% was less than PP-0% and this suggests that less charge is injected into PP-2% as compared to the other two materials. Resolving the space charge distribution in the material with the PEA technique (described below) further substantiates this hypothesis.

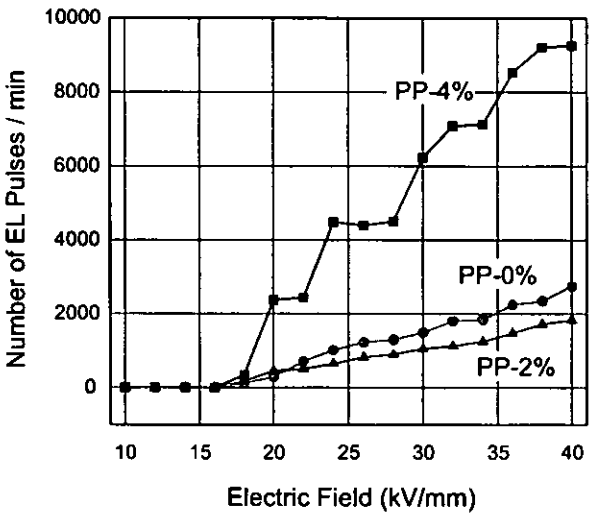

Fig. 3. EL emission in the three materials versus the applied ac field.

Fig 4 shows the space charge distribution obtained by the PEA technique in PP, containing 0, 2, and 4% by weight of nanoparticles, when charged at ac fields of 2, 20, and 30 kV/mm. To minimize the capacitive charge the space

charge was obtained at the 0° phase of the ac cycle.

As shown in the graph, no space charge was detected when charging at 2 kV/mm; but at 20 kV/mm two peaks, a positive peak at 22 μm and a negative peak at 34 μm from the low voltage electrode, appeared in all three materials. PP-2% had less space charge than the other two materials and even at maximum electric stress of 30 kV/mm (Fig. 4 b) it had the smallest peaks at 22 μm and 34 μm. This experimental evidence that PP-2% has less space charge than PP-0% and PP-4% may explain why PP-2% has the lowest EL intensity. Evidently, less charge is injected into PP-2%. The double-layer formed across the metal-polymer interface governs the charge transfer from the metal into the insulation and could be influenced by the contamination at the surface of the material.

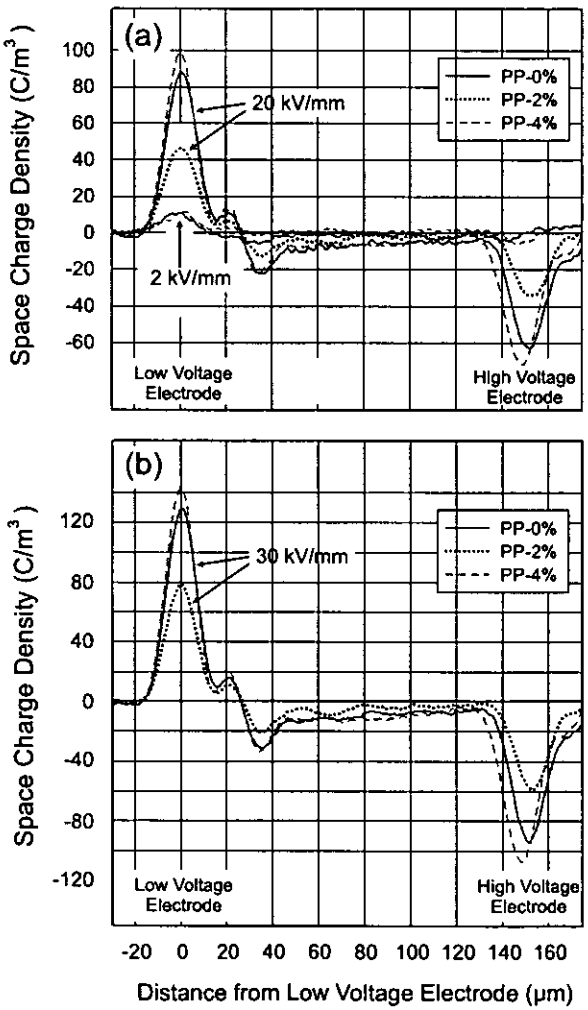

Fig. 4. Space charge distribution in PP-0%, PP-2%, and PP-4% charged at ac field of 2, 20, and 30 kV/mm.

An interesting feature of the PEA method was observed when the time dependence of the PEA signal was recorded at various phase angles of the ac voltage. PP-0% was subjected to ac field of 30 kV/mm (maximum value), and a train of 5 ns pulses was applied in steps of 15° from 0 to 360° phase angle of the ac voltage.

Fig. 5 shows the plot of the PEA voltage peak at the low voltage electrode versus the phase angle of the applied electric field. The PEA voltage peak decreased as the phase angle increased from 0 to 30°. It then reversed polarity and decreased with further increase of the phase angle until it reached a minimum at ~135°. Above 135° the PEA voltage peak increased, again reversed polarity at phase angle of ~225° and reached a maximum at ~315°. Then it started to decrease and at 360° it had a value close to that at 0°. A similar trend was observed for the voltage peak at the high voltage electrode, except that it was opposite to that at the low voltage electrode.

The phase angle at which the PEA peak changed polarity corresponds to the electric field at which space charge was detected in the material. EL was usually observed at the same or slightly higher value of the electric field. Recently [6], the field value at which EL inception occurs under ac voltage was correlated to the field required to store charge in materials subjected to ac voltage. The results were consistent with a model of electron-hole injection and recombination during each positive and negative cycle of the ac voltage.

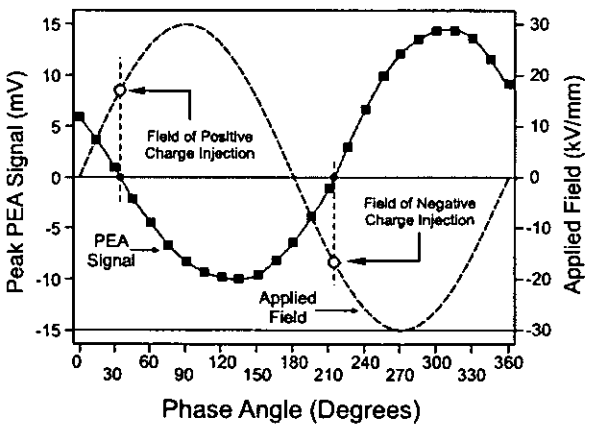

Fig. 5. PEA voltage peak at the low voltage electrode of PP-0% versus the phase angle of the applied field (dashed curve).

From Fig. 5 it can be inferred that charge injection will initiate at the electric field value at which the PEA peak reverses polarity. The injection of positive or negative charges will continue till the PEA output peak reaches its

minimum (for hole injection) or maximum (for electron injection). However, EL emission reaches its maxima prior to the peaks of the positive and negative half-cycles of the ac voltage. This is because the local electric field due presence of space charge in the polymer is always in advance of the applied field [3]. Further experimental work is required to verify this initial finding that the reversal of the PEA output voltage peak at the electrodes corresponds to the initiation of charge injection in the material. Organoclay added to PP could increase the electric field for charge injection into the polymer.

Conclusions

Dielectric properties of PP with and without organoclay are reported. PP-2% had the highest dc breakdown strength of the three materials. The results of the EL intensity and space charge distribution indicate that under ac voltage less charge is injected into PP-2% than PP-0% or PP-4%. This suggests that the electrode-polymer interface plays a dominant role during the application of ac voltage to the insulation. Phase resolved PEA technique showed that the reversal of the PEA output peak at the electrodes corresponded to the field at which charge injection into the polymeric insulation was initiated. This work has shown that PP containing 2% by weight of dispersed organosilicate has better dielectric properties, such as higher dc BD strength, less EL intensity and space charge, than pure PP.

References

[1] M. Rabuffi and G. Picci, "Status quo and future prospects for metalized polypropylene energy storage capacitors", IEEE Trans. on Plasma Science, vol.3, pp. 1939-1942, 2002.

[2] E. Ildstad and T. Haave, "Conduction and partial discharge activity in HVDC cable insulation of lapped polypropylene films", IEEE 7th Intl. Conference on Solid Dielectrics, June 25-29, 2001, pp. 137-140.

[3] K. Tohyama, S.S. Bamji, and A.T. Bulinski, "Simultaneous measurement of electroluminescence and dissipation current in cable insulation", Proc. of 7th Intl. Conf. on Properties and Applications of Dielectric Materials, June 1-5, 2003, pp. 1051-1054.

[4] L. A. Utracki, "Clay-containing Polymeric Nanocomposites", Publisher: RAPRA Tech Ltd., Shawbury, Shrewsbury, Shropshire UK, (2004).

[5] C. Laurent, "Optical pre-breakdown warnings in insulating polymers", IEEE Intl. Conference on Conduction and Breakdown in Solid Dielectrics, June 22-25, 1998, pp. 1-12.

[6] C. Laurent, G. Teyssedre, and G. C.Montanari, "Time-resolved space charge and electroluminescence measurements in polyethylene under ac stress", IEEE Trans. on Diel. and Electrical Insulation, vol. 11, pp. 554-560, 2004.

Acknowledgments: Mrs. Y. Chen and Mr. D. McIntyre provided technical assistance to this project. Mr. D. St-Jean machined various test-cells and other experimental setup components and Dr. Jianming. Li (from NRCC/IMI) provided the nanocomposite samples. Their assistance is very much appreciated.

Author's Address: Soli Bamji INMS, National Research Council Canada, 1200 Montreal Road, Ottawa, Ontario, Canada K1A 0R6 Email: soli.bamji@nrc-cnrc.gc.ca

Dielectric Properties of Polypropylene Containing Nano-Particles

S.S. Bamji, M. Abou-Dakka, and A.T. Bulinski
Institute for National Measurement Standards
National Research Council Canada
Ottawa, Ontario, Canada, K1A 0R6

L. Utracki and K. Cole
Industrial Materials Institute
National Research Council Canada
Boucherville, Quebec, Canada, J4B 6Y4

Abstract: A thermoplastic such as polypropylene reinforced with small quantities (<5% by weight) of nano-sized particles could show reduced flammability as well as improved dielectric properties. This paper describes short-term dielectric properties of polypropylene containing 0%, 2%, and 4% by weight of dispersed organosilicates. Ac and dc breakdown strength, tanδ, electroluminescence emission, and space charge distribution due to ac poling of polypropylene with and without the nanoparticles are reported.

Introduction

Polypropylene (PP) is extensively used as a dielectric material in power capacitors and cable wraps, as well as in layer and phase separators for rotating electrical equipment and transformers [1, 2]. It has excellent mechanical, thermal, and electrical properties and provides outstanding resistance to moisture, grease, and oils. PP does not present stress-cracking problems and compared to polyethylene it offers excellent electrical and chemical resistance at higher temperatures.

Incorporation of nanoparticles in a polymer matrix could provide dielectrics with new and improved properties. A thermoplastic such as PP could be reinforced with small quantities (<5% by weight) of nanoparticles. This could enhance the mechanical properties and flame resistance and may improve dielectric properties, such as long-term electrical breakdown strength, surface and volume conductivity and resistance to partial discharges.

This paper describes dielectric properties of PP during short-term electrical aging and compares them with PP containing dispersed nanoparticles. Breakdown strength, dielectric loss at power frequency, electroluminescence emission, and space charge distribution in these materials are compared and discussed.

Experimental

Sample Preparation: Three materials, isotactic PP with 0, 2, and 4-wt% of organosilicate, referred to in this text as PP-0%, PP-2%, and PP-4%, were used. The manufacture of polypropylene containing nanoparticles involved two new methods:

(1) Melt compounding of PP (ProFax PDC 1274 from Basell), with a 1:1 mixture of two compatibilizers [PP grafted with maleic-anhydride (PP-MA) from Eastman (Epolene-3015) and from Crompton (Polybond 3150)] and organoclay (Cloisite 15A, C15A, from SCP). The compounding was carried out under a blanket of dry nitrogen in a twin-screw extruder with a gear pump and an extensional flow mixer (EFM, gap = 63.5 μm, throughput Q = 10 kg/h) at 200°C. The resulting composition was: 88-wt%PP + 8-wt%PP-MA + 4-wt%C15A (referred to as PP-4%). The organoclay dispersion of PP-4% was characterized by X-ray diffraction (XRD) and high-resolution transmission electron microscopy (HRTEM). The interlayer spacing was d_{001} = 3.25 nm; the number of clay platelets in residual stacks N = 3.25, and the degree of exfoliation = 79%, i.e., 11% above that observed for extrusion without the EFM.

(2) The same materials were melt compounded using a combination of a single screw extruder and EFM (with 15 μm gap, 10 kg/h throughputs) at 180°C, under blanket of dry nitrogen. The composition of the compound was 92-wt%PP + 4-wt%PP-MA + 2-wt%C15A (referred to as PP-2%). The organoclay dispersion of PP-2% was characterized by XRD and HRTEM. The measured dispersion parameters were: d_{001} =3.45 nm, N = 2.64, and degree of exfoliation 20% above that observed for extrusion without EFM.

The three materials were molded using a hot press at 210°C under a pressure of 50 MPa to produce flat sheets having a thickness of 80±5 μm and 155±5 μm. The thinner samples were used to determine the light transmission characteristics, and then they were subjected either to ac or dc breakdown tests or used for tanδ measurements. The thicker samples had each of

their sides sputtered with gold electrodes having a diameter and thickness of 25 mm and 30 nm respectively and then used for electroluminescence and PEA measurements.

UV-VIS-NIM Spectra: The light transmission spectra of each of the three materials were obtained with a UV- VIS-NIR Perkin-Elmer spectrometer having a range of 160 nm to 3200 nm.

Breakdown (BD) Tests: The samples were placed between two electrodes inside an oil bath. The bottom circular electrode having a diameter larger than that of the sample was held at ground potential. The top electrode, connected to a high voltage supply, had a diameter much smaller than that of the sample so that several breakdowns could be obtained on each sample. For dc tests the positive voltage was increased at a rate of 90 V/s, while for ac tests the voltage was increased at a rate of 70 V/s till breakdown occurred. RMS values of ac voltage and field are used throughout this paper.

Tanδ and Capacitance: Andeen Hagerling Ultra-precision Capacitance Bridge operating at 15 V, 60 Hz was used to obtain tanδ and measure the capacitance of each sample.

Electroluminescence (EL): The setup for EL has been previously described [3]. An optical system was designed to capture EL from each sample subjected to ac voltage under uniform field geometry. Light emitted from only the central region of the sample was detected by a PMT operating in photon counting mode. EL emitted at any phase, from 0 to 360°, during each cycle of the ac voltage could be detected by the system. The electric field was increased from 0 to 40 kV/mm in steps of 2 kV/mm.

Phase Resolved PEA Technique: Space charge distribution in the sample during ac aging was obtained with a PEA system from FiveLabs, Japan. A constant pressure was maintained during the measurement and the spatial resolution of the system was ~10 μm. The sample was electrically stressed with ac voltage and special software was developed to synchronize the pulse generator with the high voltage supply to provide a train of 5 ns pulses during any phase angle, between 0 to 360°, of the ac voltage. The pulses with amplitude of 200 V were applied for 1000 consecutive cycles of the ac voltage. The average of several hundred repetitive measurements was obtained to improve the signal to noise ratio. The PEA signal was digitized at a rate of 10 GS/s by a fast digital oscilloscope and each data point was resolved at 100 ps.

Results and Discussion

The optical transmission of the three materials in the 160-3200 nm range is shown in Fig. 1. Between 200 nm and 300 nm (see inset) the transmission decreases as the nanoparticle content increases. This could be attributed to silicate and intercalate used in the nanocomposites. The apparent gradual decrease in transmission as the wavelength decreases from 2200 to 300 nm is mainly related to scattering, which increases as the wavelength gets closer to the dimensions of the scattering clay platelets. Much of the scattered light may actually be transmitted, but because it falls outside of the angle detected by the spectrometer, it appears as loss of transmission (or caused by absorption). For wavelengths above ca. 300 nm the scattering is significantly higher for PP-0% than for the nanocomposites, and this is almost certainly related to the size of the PP crystalline domains (spherulites). The spherulites have a different index of refraction from the amorphous regions, which leads to reflection of light at the interface and hence to scattering. The organoclay acts as a nucleating agent; hence it increases the number of spherulites and reduces their size, which shifts the scattering drop-off to shorter wavelength. In the near IR, the peak at 2750 nm arises from the fundamental OH stretching vibration of the hydroxyl groups contained within the silicate layers. As expected, its intensity is proportional to the amount of clay.

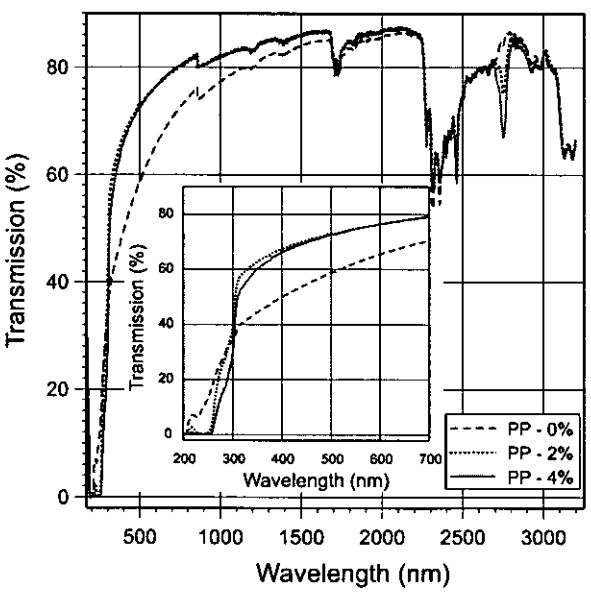

Fig. 1. UV-VIS-NIR transmission spectra of polypropylene containing 0, 2, and 4% by weight of organoclay.

The dc and ac BD strength of the three materials and the error of measurements are presented in Fig. 2.

The graph shows the average value of at least ten breakdowns for each material. Adding organoclay to PP increases the dc breakdown strength. Silicate layers are known to be efficient nucleating agents for crystallization of PP matrix. Charges could be trapped at the nanofiller-polymer matrix interfaces and thus decrease the probability of breakdown. For the three materials tested in this work, PP-2% had the highest breakdown strength, as shown in Fig. 2. The slightly lower ac and dc BD strength of PP-4%, as compared to PP-2%, could be due to the decrease in spherulite size and density and poorer dispersion of the nanoparticles.

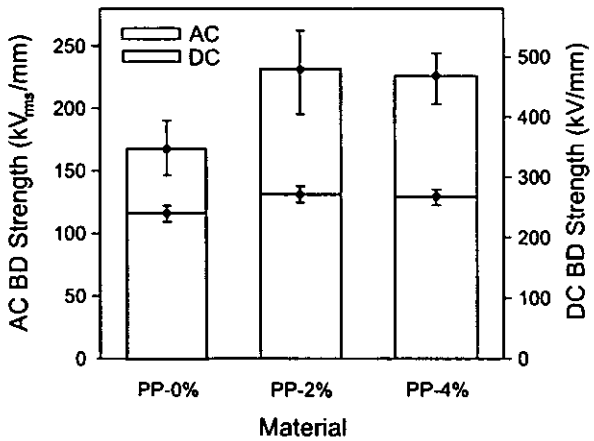

Fig. 2. AC and DC breakdown values of PP containing 0, 2, and 4% of nanoparticles

Tanδ and capacitance values at 15 V and 60 Hz of the three materials are listed in Table 1. Adding organoclay increases the tanδ of PP by an order of magnitude and PP-4% has twice the value of PP-2%. The capacitance also increases with the concentration of the nanofiller content. In the maleated PP the maleic anhydride groups are partially hydrolyzed, thus acidic and highly polar. The organoclay is montmorillonite with Fe^{+3} in the octahedral layer, and negative charges on the surface, ionically bonded to ammonium intercalant [4].

Table1. Tanδ and Capacitance values of PP, with and without nanofillers.

Material	Tanδ (x10^{-4})	Capacitance (pF)
PP-0%	1.88	123.33
PP-2%	20.1	138.97
PP-4%	42.8	146.70

According to molecular modeling the charge is highly delocalized, thus again polar, with the degree of polarity expected to be frequency dependent. These polar species increase the loss factor of the nanocomposites.

Fig. 3 shows typical EL emission from the three materials subjected to ac voltage. At least five samples of each material were tested. Adding organoclay to PP does not increase the EL inception field (~18 kV/mm) but, compared to PP-0%, the EL intensity was usually lower in PP-2% and higher in PP-4%. At low electric field, EL emission in polyolefin is caused by the recombination of electrons and holes injected into the insulating material subjected to ac voltage [3]. Enone and poly-(enone) sequences have been identified as luminescent centers in PP [5]. These polar species have equal affinity for electrons and holes and act as recombination centers for the charges of both polarities injected into the material. In the nanocomposites, the nanoparticles could provide additional recombination centers and this would increase the intensity of EL emission as in PP-4%. However, the EL intensity of PP-2% was less than PP-0% and this suggests that less charge is injected into PP-2% as compared to the other two materials. Resolving the space charge distribution in the material with the PEA technique (described below) further substantiates this hypothesis.

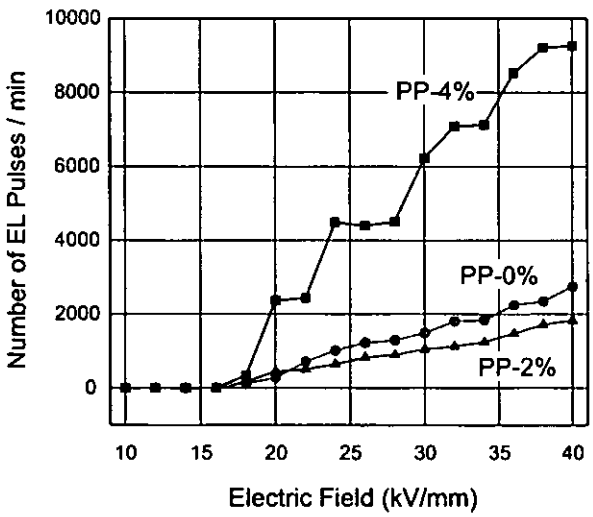

Fig. 3. EL emission in the three materials versus the applied ac field.

Fig 4 shows the space charge distribution obtained by the PEA technique in PP, containing 0, 2, and 4% by weight of nanoparticles, when charged at ac fields of 2, 20, and 30 kV/mm. To minimize the capacitive charge the space

charge was obtained at the 0° phase of the ac cycle.

As shown in the graph, no space charge was detected when charging at 2 kV/mm; but at 20 kV/mm two peaks, a positive peak at 22 μm and a negative peak at 34 μm from the low voltage electrode, appeared in all three materials. PP-2% had less space charge than the other two materials and even at maximum electric stress of 30 kV/mm (Fig. 4 b) it had the smallest peaks at 22 μm and 34 μm. This experimental evidence that PP-2% has less space charge than PP-0% and PP-4% may explain why PP-2% has the lowest EL intensity. Evidently, less charge is injected into PP-2%. The double-layer formed across the metal-polymer interface governs the charge transfer from the metal into the insulation and could be influenced by the contamination at the surface of the material.

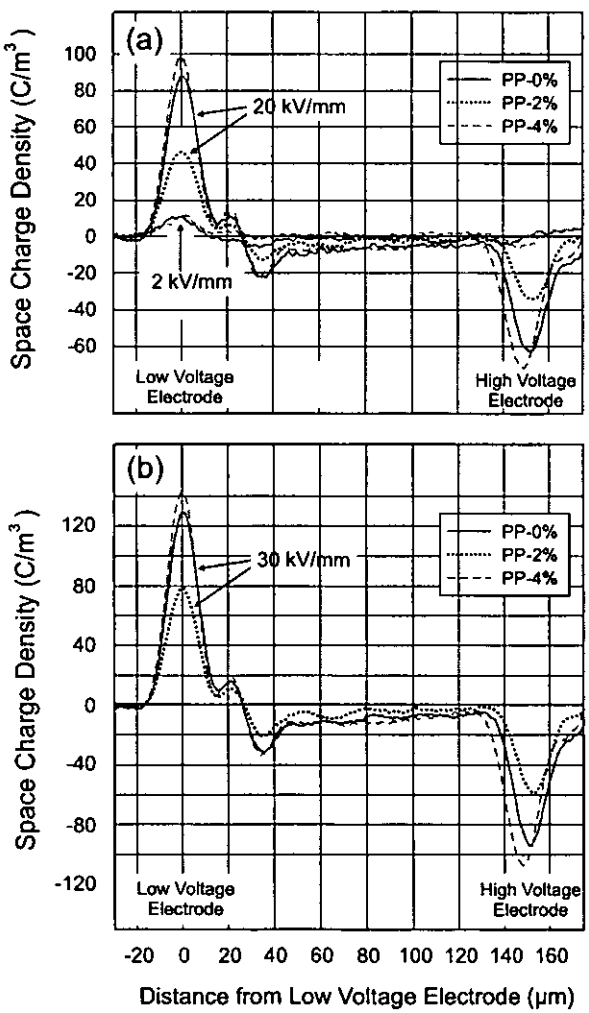

Fig. 4. Space charge distribution in PP-0%, PP-2%, and PP-4% charged at ac field of 2, 20, and 30 kV/mm.

An interesting feature of the PEA method was observed when the time dependence of the PEA signal was recorded at various phase angles of the ac voltage. PP-0% was subjected to ac field of 30 kV/mm (maximum value), and a train of 5 ns pulses was applied in steps of 15° from 0 to 360° phase angle of the ac voltage.

Fig. 5 shows the plot of the PEA voltage peak at the low voltage electrode versus the phase angle of the applied electric field. The PEA voltage peak decreased as the phase angle increased from 0 to 30°. It then reversed polarity and decreased with further increase of the phase angle until it reached a minimum at ~135°. Above 135° the PEA voltage peak increased, again reversed polarity at phase angle of ~225° and reached a maximum at ~315°. Then it started to decrease and at 360° it had a value close to that at 0°. A similar trend was observed for the voltage peak at the high voltage electrode, except that it was opposite to that at the low voltage electrode.

The phase angle at which the PEA peak changed polarity corresponds to the electric field at which space charge was detected in the material. EL was usually observed at the same or slightly higher value of the electric field. Recently [6], the field value at which EL inception occurs under ac voltage was correlated to the field required to store charge in materials subjected to ac voltage. The results were consistent with a model of electron-hole injection and recombination during each positive and negative cycle of the ac voltage.

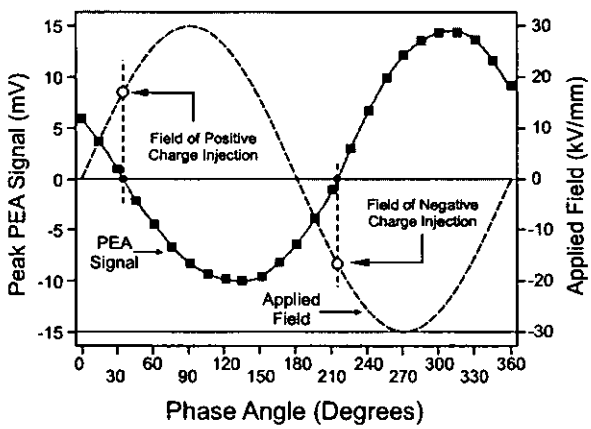

Fig. 5. PEA voltage peak at the low voltage electrode of PP-0% versus the phase angle of the applied field (dashed curve).

From Fig. 5 it can be inferred that charge injection will initiate at the electric field value at which the PEA peak reverses polarity. The injection of positive or negative charges will continue till the PEA output peak reaches its

minimum (for hole injection) or maximum (for electron injection). However, EL emission reaches its maxima prior to the peaks of the positive and negative half-cycles of the ac voltage. This is because the local electric field due presence of space charge in the polymer is always in advance of the applied field [3]. Further experimental work is required to verify this initial finding that the reversal of the PEA output voltage peak at the electrodes corresponds to the initiation of charge injection in the material. Organoclay added to PP could increase the electric field for charge injection into the polymer.

Conclusions

Dielectric properties of PP with and without organoclay are reported. PP-2% had the highest dc breakdown strength of the three materials. The results of the EL intensity and space charge distribution indicate that under ac voltage less charge is injected into PP-2% than PP-0% or PP-4%. This suggests that the electrode-polymer interface plays a dominant role during the application of ac voltage to the insulation. Phase resolved PEA technique showed that the reversal of the PEA output peak at the electrodes corresponded to the field at which charge injection into the polymeric insulation was initiated. This work has shown that PP containing 2% by weight of dispersed organosilicate has better dielectric properties, such as higher dc BD strength, less EL intensity and space charge, than pure PP.

References

[1] M. Rabuffi and G. Picci, "Status quo and future prospects for metalized polypropylene energy storage capacitors", IEEE Trans. on Plasma Science, vol.3, pp. 1939-1942, 2002.

[2] E. Ildstad and T. Haave, "Conduction and partial discharge activity in HVDC cable insulation of lapped polypropylene films", IEEE 7th Intl. Conference on Solid Dielectrics, June 25-29, 2001, pp. 137-140.

[3] K. Tohyama, S.S. Bamji, and A.T. Bulinski, "Simultaneous measurement of electroluminescence and dissipation current in cable insulation", Proc. of 7th Intl. Conf. on Properties and Applications of Dielectric Materials, June 1-5, 2003, pp. 1051-1054.

[4] L. A. Utracki, "Clay-containing Polymeric Nanocomposites", Publisher: RAPRA Tech Ltd., Shawbury, Shrewsbury, Shropshire UK, (2004).

[5] C. Laurent, "Optical pre-breakdown warnings in insulating polymers", IEEE Intl. Conference on Conduction and Breakdown in Solid Dielectrics, June 22-25, 1998, pp. 1-12.

[6] C. Laurent, G. Teyssedre, and G. C.Montanari, "Time-resolved space charge and electroluminescence measurements in polyethylene under ac stress", IEEE Trans. on Diel. and Electrical Insulation, vol. 11, pp. 554-560, 2004.

Acknowledgments: Mrs. Y. Chen and Mr. D. McIntyre provided technical assistance to this project. Mr. D. St-Jean machined various test-cells and other experimental setup components and Dr. Jianming. Li (from NRCC/IMI) provided the nanocomposite samples. Their assistance is very much appreciated.

Author's Address: Soli Bamji INMS, National Research Council Canada, 1200 Montreal Road, Ottawa, Ontario, Canada K1A 0R6 Email: soli.bamji@nrc-cnrc.gc.ca